POAC'15
Trondheim, Norway

Proceedings of the 23rd International Conference on
Port and Ocean Engineering under Arctic Conditions
June 14-18, 2015
Trondheim, Norway

STATION KEEPING IN ICE - ICE TANK EXPERIMENT AND ESTIMATION OF ICE LOAD ON SHIP-SHAPED FLOATING STRUCTURE UNDER MANAGED ICE CONDITION-

Shotaro Uto[1], Takatoshi Matsuzawa[1], Haruhito Shimoda[1], Daisuke Wako[1]
Akihisa Konno[2], Takayuki Asanuma[3] and Kazuhisa Otsubo[3]
[1]National Maritime Research Institute, Tokyo, Japan
[2]Kogakuin University, [3]Japan Oil, Gas and Metals National Corporation

ABSTRACT

In order to find the feasibility of the Arctic drilling and developments using floating offshore structures, we conducted the research on ice loads in managed ice condition exerted on the ship-shaped floater by experiment and numerical simulation. The experiment was conducted at the ice model basin of the National Maritime Research Institute, Japan. Through the comparison with experiment results, it was found that the numerical simulation was capable of predicting ice load qualitatively well. It showed good agreement for the surge force and predicted the same order of sway force. Finally, a simple prediction formula was established for the average surge and sway force, and yaw moment. Its accuracy was validated by the experimental data.

NOMENCLATURE

B:	Ship breadth
C:	Concentration of ice (0: ice free, 1.0: fully ice-covered)
C_{WE}:	Waterline coefficient at the forward part of the ship
d_i:	Floe size (diameter of circular floe with the same area)
F_L:	Froude number based on ship length
F_x:	Surge force
F_y:	Sway force
h_i:	Thickness of ice (including snow depth)
L:	Ship waterline length
L_H:	Length from stem to parallel part of the mid-body
M_z:	Yaw moment
v:	Ice drift speed
α:	Waterline entrance angle
θ:	Ice drift angle
ϕ:	Stem angle

φ: Angle between the normal of the surface and a vertical vector
μ: Friction coefficient between hull and ice
ρ: Density
Suffix
i: Ice
o: Values at the stem
w: Water

INTRODUCTION

Dynamic positioning in ice is one of the most critical issues for the successful Arctic operation such as drilling. In particular, prediction of ice loads is one of the most challenging issues and experimental and numerical works have been conducted recently. Haase et al. (2013) introduced DYPIC (Dynamic Positioning in Ice) project and the model-scale experiment at the ice model basin to evaluate ice loads and performance of the DP system. They conducted both fixed and free-running model tests in various ice conditions and discussed the relation between ice loads and ice conditions. Jensen et al. (2009) reported that the turning moment from ice may be either stabilising or destabilising the vessel heading and shows significant change in time.

Regarding numerical modeling of ice resistance in floe ice, Metrikin et al. (2012) proposed the numerical simulation method of a floater in a broken ice field by publicly available physics engines. Konno et al. (2013) developed the numerical method of resistance in a brash ice channel based on the physically based modeling. Kerkeni et al. (2013) used a physically based time-domain simulator to make capability plots of dynamic positioning in ice. Physically-based modelling is one of the most promising methods in this field.

Understanding the physical mechanism is limited on the forces and moment exerted on the drillship in ice DP operation. In this regard, the mathematical work is indispensable. However few works have been done so far (for example, Bakkay, Coche and Riska, 2014).

We conducted the experimental, numerical and mathematical works on the ice load for ships in managed ice condition. In the experimental works, both ice load measurement and DP experiments are conducted for the ship-shaped floater in managed ice conditions. Numerical simulation is conducted based on the physically based modeling. The mathematical expressions of the average ice forces and yaw moment are developed by extending the formula of resistance in small ice floes. Measured forces and moment in the fixed experiments are used for the validation of the numerical and mathematical works.

EXPERIMENT

Ice Model Basin

Ice load measurements using the scaled-model of drillship were conducted at the ice model basin of the National Maritime Research Institute, Japan. Figure 1 and Table 1 show the section view of the ice model basin and specifications, respectively.

Model Ship

Table 2 shows the principal dimensions of the drillship. The model-to-ship scale ratio is 70. Figure 2 shows the photo of the model.

Ice Conditions

In order to simulate the managed ice condition, an ice sheet is cut into pieces with rectangular and triangular shapes (Figure 3). The area of the floe varies between 0.02 and 0.16 m^2. The

diameter of the circular disk with the same area is between 0.16 to 0.45m, corresponding to between 11 and 32m in full scale. Keinonen et al. (2006) reported that average floe sizes of 10 to 20m were observed with maximum floe sizes of 20 to 40m during the coring operation in the central Polar Pack. The floe size in full scale is almost identical with the observed size.
Target ice thicknesses are 0.0143m, 0.025m and 0.0357m. In full scale, they correspond to 1.0m, 1.75m and 2.5m, respectively. Ice concentration is around 0.8 in the first test run. Ice concentration decreases gradually by removing some ice floes. In this experiment, the range of ice concentration is from 0.84 to 0.66.

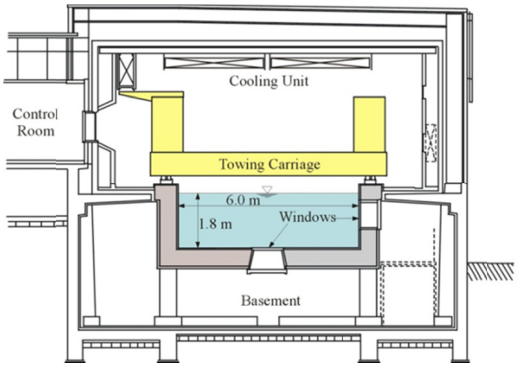

Figure 1. Ice model basin

Table 1. Specifications of ice model basin

Length	m	35.0
Breadth	m	6.0
Water depth	m	1.8
Freezing rate	mm/h	2 - 3

hip

Item		unit	Ship	Model
Length between perpendiculars	L_{pp}	m	200.0	2.86
Breadth	B	m	38.0	0.54
Draft	d	m	16.5	0.24
Depth molded	D	m	23.4	0.33
Displacement	W	m^3	102980.8	0.30

Figure 2. Photo of model drillship

Figure 3. Managed ice condition

Measurement Methods and Test Conditions

Tests were conducted in fixed and free-running modes. In this paper, we report the results of fixed model tests. The model is fixed to the carriage and towed at the constant speed. Ice load exerted on the hull of the model drillship is measured by 6-component load cell. The behavior

of ice floes is recorded by the motion picture through the observation windows at the side and bottom of the basin (see Figure 1). Ice pressure on the hull is measured by the pressure measurement system (Izumiyama et al., 2005).
A time history of the ice fraction is obtained by image-thresholding a transverse line in an image taken in front of the model. The representative ice concentration is calculated as its average. In order to simulate the ice flow, the model drillship is towed with a drift angle by the towing carriage. The speed is 0.031, 0.062 and 0.092m/sec, which correspond to 0.5, 1.0 and 1.5 knot in full scale. The ice drift angle is between 0 and ±15 degrees in most cases.

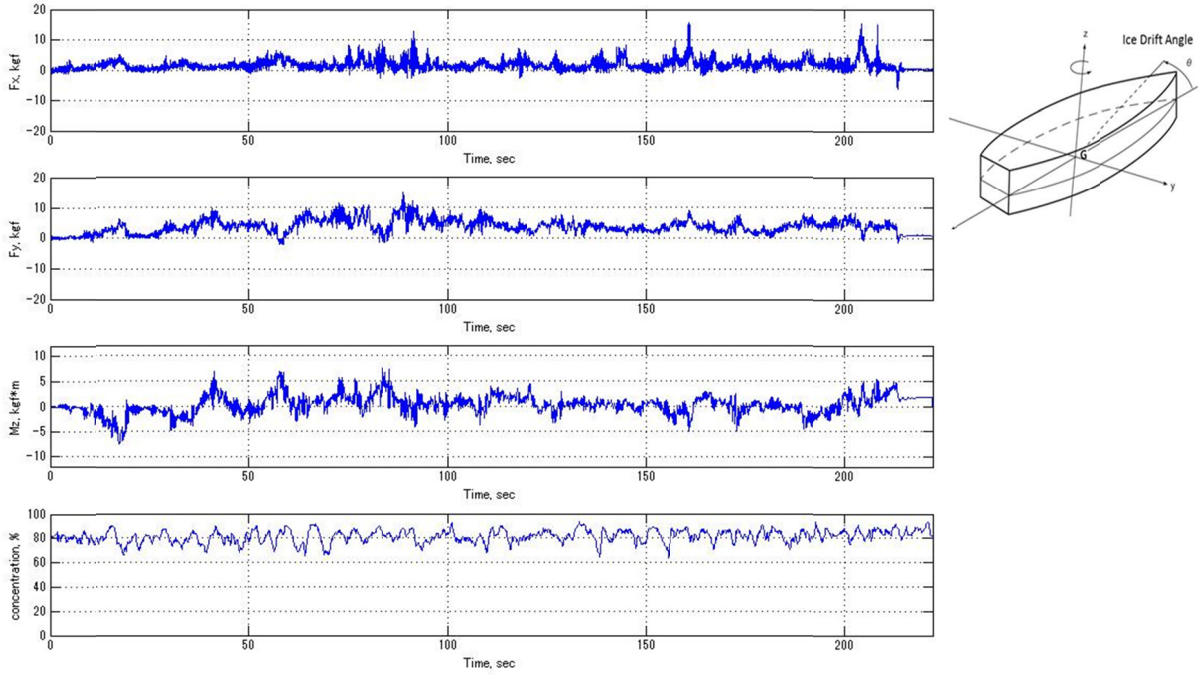

Figure 4. Time histories of surge and sway forces, yaw moment and ice concentration (h_i=0.0371m, C= 0.82, v=0.061m/sec, θ=10 degree)

Results

Results of ice load measurements are reported in this paper. Figure 4 shows the example of time histories of surge (F_x) and sway forces (F_y), yaw moment (M_z) and ice concentration. As reported in the previous papers (For example, Jensen et al., 2009), significant change of yaw moment is observed in its time history.

NUMERICAL SIMULATION BY PHYSICALLY BASED MODELLING

Simulation Methods and Materials

To simulate ship navigation in an ice field, it is necessary to address collisions and other mutual interactions among ice pieces and the ship. We incorporate physically based modeling into our simulation program to handle that situation. Detailed description of the simulation method is in Konno et al. (2013).
In this study, we simulate model experiments described in the previous section. Initial arrangements of ice pieces are generated corresponding to the model experiments, as depicted in Figures 5 and 6. These arrangements are generated on the following conditions.
In each case, the width and length of the channel are set to 6 m and 28 m, respectively. The channel consists of two kinds of square ice (large and small), and two kinds of disc ice (large and small). The sizes of square ice pieces are the same as those of the model experiments. The sizes of the disc ice are decided so that the areas of the ice pieces are the same as those of the

model experiment. Therefore, the lengths of the edges of the large and small square ice pieces are 0.3m and 0.15m, respectively, and the radii of the large and small disc ice pieces are 0.223 m and 0.1114 m, respectively.

In the process of generating initial ice condition, ice pieces are systematically generated so that the number ratio of large square ice, small square ice, large disc ice and small disc ice becomes 3:4:2:4. After that, the ice pieces that protruded the analysis region are deleted.

In each initial condition, thickness of ice pieces is unique. In this paper we report results with ice thickness 0.024 m.

We prepared ice conditions with five different concentrations: 0.60, 0.65, 0.70, 0.75 and 0.80. Figure shows the initial arrangements of ice pieces with concentration of 0.80. In this paper we report results with concentrations of 0.65 and 0.80. Other conditions for simulations are described in Table 3.

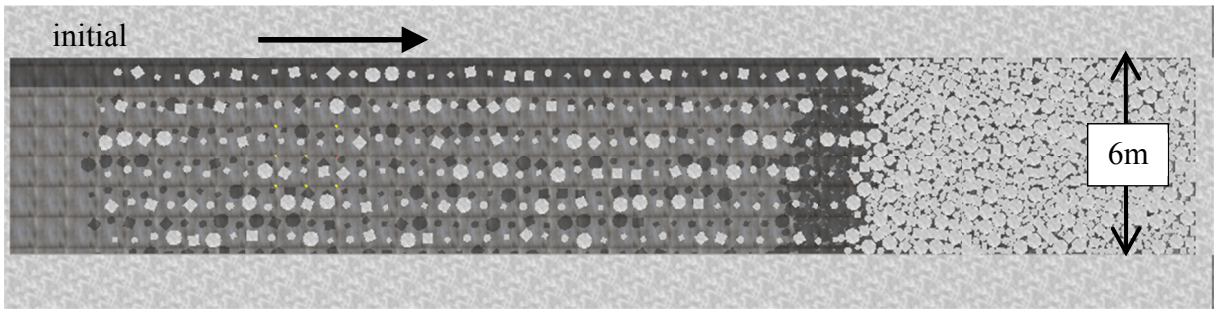

Figure 5. Generation method for initial ice condition

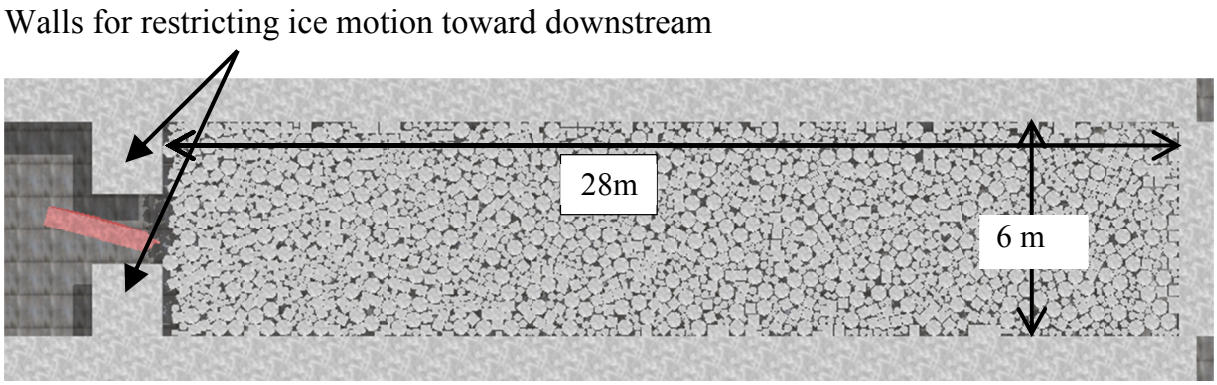

(a) Top view

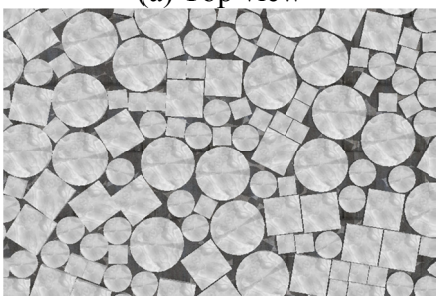

(b) Enlarged view

Figure 6. Initial ice placement

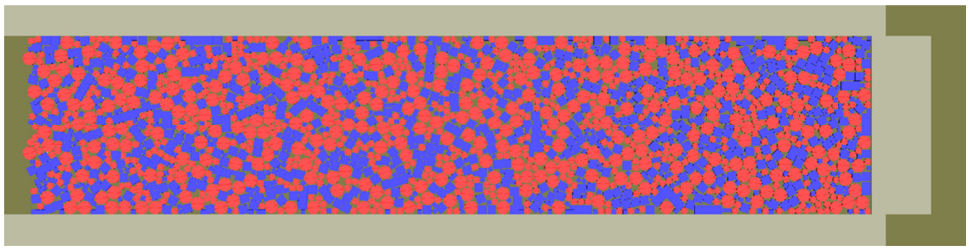

C=0.80, number of ice pieces: 2149

Figure 7. Top view of initial ice arrangements. red: circular piece, blue: rectangular piece

Table 3. Simulation conditions

density of water	1000 kg/m^3
density of ice	900 kg/m^3
ship speed	0.0615 m/s (1.0 kt in real scale)
yaw angle of ship	0, 5, 10 and 15 deg.
friction coefficient (ship-ice)	0.15
friction coefficient (ice-ice)	0.1
drag coefficient of ice pieces	1.0
coefficient of restitution	0
time step	0.01 s

Simulation Results

A snapshot of the situation is depicted in Figure 8. In the numerical analyses, un-physical phenomena, like the piece of ice intersects into the ship hull have not occurred. On the other hand, un-physical intersection between ice pieces is observed in some cases. These do not occur often (ex: a few in case of 2000 ice pieces) and intersection often occurs in the direction of thickness. Therefore we judged that we can safely ignore these intersections.

Examples of calculated ice loads are depicted in Figure 9. In the case with concentration 0.80, the simulation reproduces the tendency of the forces; the force first gradually increases but later becomes constant with fluctuations.

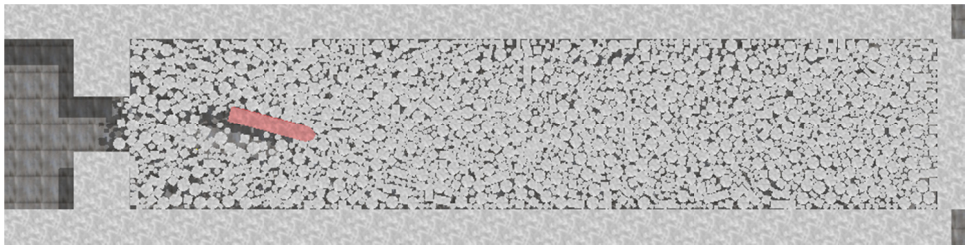

Time: 50 s

Figure 8. Snapshot of numerical simulation. h_i= 0.024 m, C=0.80, θ=15 deg., v= 0.0615 m/s

Average ice loads between 100 s and 200 s are calculated from these analyses, and these averages are compared with the experimental results as depicted in Figure .

From this figure it is observed that the simulation successfully reproduces the qualitative relationship of surge or sway forces and yaw angles. Surge forces do not have a clear correlation with yaw angles, while sway forces have a positive correlation with yaw angles.

In cases of concentration 0.65, surge forces agree well each other. In cases of 0.80, surge forces are close, but the simulation slightly overestimates the sway force.

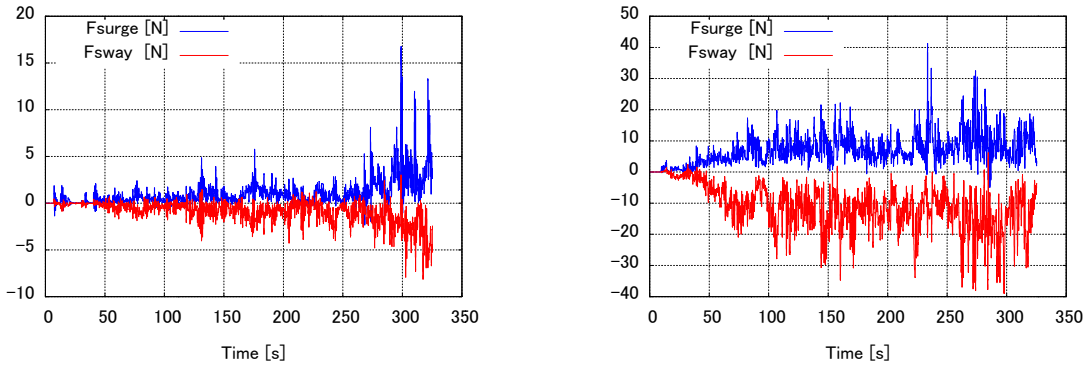

Figure 9. Time histories of ice loads. h_i= 0.024 m, θ=15 deg., v= 0.0615 m/s s

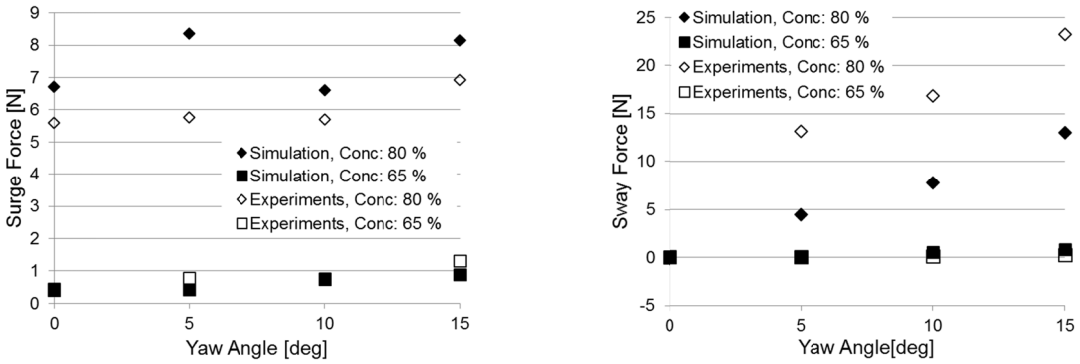

Figure 10. Surge and sway forces in numerical simulation and model experiments with different yaw angles

Sway forces in the simulation also agrees well with those of the model experiments in cases of concentration 0.65. In cases of concentration 0.80, the simulation underestimates the sway force about 10 N. In the model test, the ratio of surge and sway forces is 1 to 3, while the ratio in the simulation is 1 to 2.

From these results, we conclude this simulation method is promising approach to provide the information for considering a design and operation of a drillship.

SIMPLE ANALYTICAL FORMULA

In this section, we developed a simple analytical formula to predict surge, sway forces and yaw moment for ships operating in managed ice floes. We extended the model by Kashitelijan, Poznjok and Ryblin (Nozawa, 2006) which was originally developed as the resistance model in small ice floes. This model assumes ice forces as the sum of impact, dissipative and static components. No failure and submergence of ice floes are taken into account in this model. Uto et al. (2015) showed the validity of the original model by comparing the results by model and full-scale measurements.

Ice Force in Surge Direction

$$F_{Surge} = F_{Surge1} + F_{Surge2} + F_{Surge3} \tag{1}$$

$$F_{Surge1} = \frac{1}{2}\bar{k}_3 \rho_i g d_i h_i L F_L^2 (\tan^2(\alpha_0 + \theta) + \tan^2(\alpha_0 - \theta)) \tag{2}$$

$$F_{Surge2} = \frac{1}{2}\bar{k}_2 \rho_i g d_i h_i F_L \left[B_1(\mu + C_{WE1}(\tan\alpha_0 + \theta)) + B_2(\mu + C_{WE2}(\tan\alpha_0 - \theta))\right] \quad (3)$$

$$F_{Surge3} = \frac{1}{2}\bar{k}_1 \rho_i g \sqrt{d_i h_i}\left[(\frac{B_1}{2})^2(1 + 4\mu C_{WE1}\frac{L_{H1}}{B_1}) + (\frac{B_2}{2})^2(1 + 4\mu C_{WE2}\frac{L_{H2}}{B_2})\right] \quad (4)$$

Here, $\bar{k}_1$, $\bar{k}_2$ and $\bar{k}_3$ are empirical constants. $\bar{k}_1$ and $\bar{k}_2$ are the function of ice concentration and expressed approximately in equation (5) by 2nd order-polynomial curve fitting.

$$\bar{k}_1 = 0.25C^2 - 0.215C + 0.039, \quad \bar{k}_2 = 9.63C^2 - 1.20C \quad (5)$$

Table 4 Parameters of KPR Model

C	0.4	0.6	0.8	1.0
$\bar{k}_1$	0	0	0.027	0.074
$\bar{k}_2$	0.93	2.54	5.70	8.20
$\bar{k}_3$	4.30	4.30	4.30	4.30

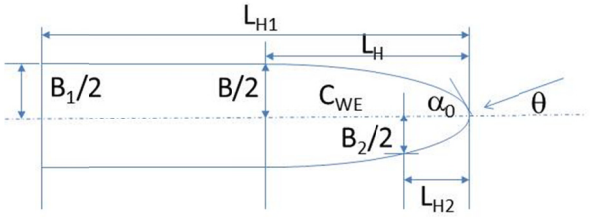

Figure 5. Definition of ship parameter

Ice Force in Sway Direction

$$F_{Sway} = F_{Sway1} + F_{Sway2} + F_{Sway3} \quad (6)$$

$$F_{Sway1} = \frac{1}{2}\bar{k}_3 \rho_i g d_i h_i L \mu F_L^2(\tan^2(\alpha_0 + \theta) - \tan^2(\alpha_0 - \theta)) \quad (7)$$

$$F_{Sway2} = \frac{1}{2}\bar{k}_2 \rho_i g d_i h_i F_L \left[B_1(1 + \mu C_{WE1}(\tan\alpha_0 + \theta)) - B_2(1 + \mu C_{WE2}(\tan\alpha_0 - \theta))\right] \quad (8)$$

$$F_{Sway3} = \frac{1}{2}\bar{k}_1 \rho_i g \sqrt{d_i h_i}\left[(\frac{B_1}{2})^2(\mu + 4C_{WE1}\frac{L_{H1}}{B_1}) - (\frac{B_2}{2})^2(\mu + 4C_{WE2}\frac{L_{H2}}{B_2})\right] \quad (9)$$

Yaw Moment

Estimation of yaw moment is one of the most challenging technical issues for realization of dynamic positioning in ice. Figure 12 indicates the relation of the average values between yaw moment and sway force. The vertical axis is the normalized lever of yaw moment (L_{Mz}) calculated by equation (10).

$$L_{Mz} = M_z / F_{Sway} / L_{pp} \quad (10)$$

In the present study, we propose the simple formula for the average value of yaw moment by equation (11). Here sway force is calculated by equations (6) to (9).

$$M_z = 0.2 F_{Sway} L_{pp} \quad (11)$$

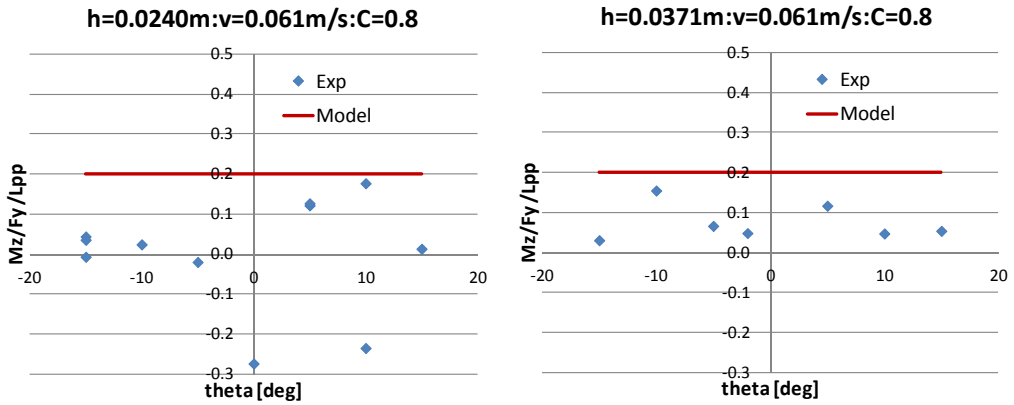

Figure 6. Lever of yaw moment vs. drift angle

Verification of the model

Accuracy of the proposed model is verified by comparing with the measured forces and moment. For simplicity, we assume $C_{WE1} = C_{WE2} = C_{WE}$ in equations (8) and (9).

Figure 13 shows the comparison of surge (left column) and sway (right) forces between measurements and prediction.

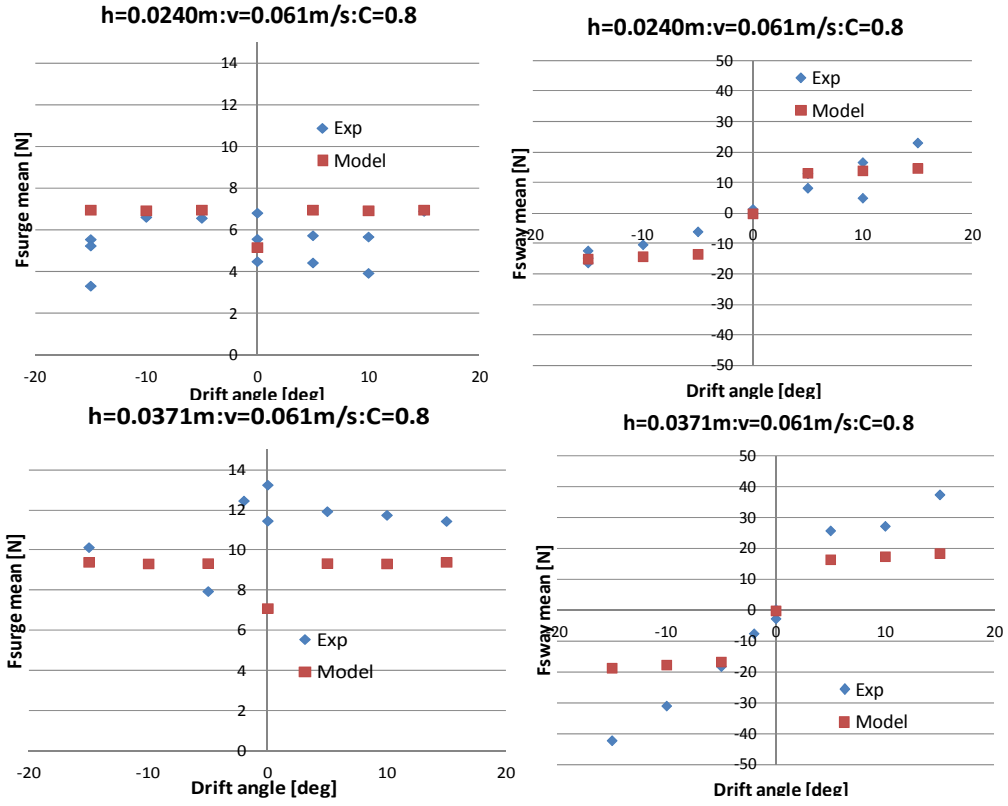

Figure 7. Comparison of surge and sway forces between measurements and predictions -1

Measured ice forces are obtained by subtracting the forces measured in ice-free water from the total forces in ice. Reasonable agreement is obtained on the dependency of ice forces on the drift angle. Surge force is almost constant and sway force increases as the drift angle increases. Discontinuous change of the predicted sway force around θ=0 is due to the large change of L_H against the drift angle.

Figure 8 shows the comparison of ice forces in terms of the dependency of ice thickness. It is observed that both of measured and predicted ice forces increases as the ice thickness. However the increase rate is small in the model compared to the measurement data. The present model predicted higher forces at the thinner ice and lower forces at the thicker ice.

Figure 9 shows the comparison of yaw moment between measurements and prediction. It is found that reasonable agreement is obtained by the present simple formula.

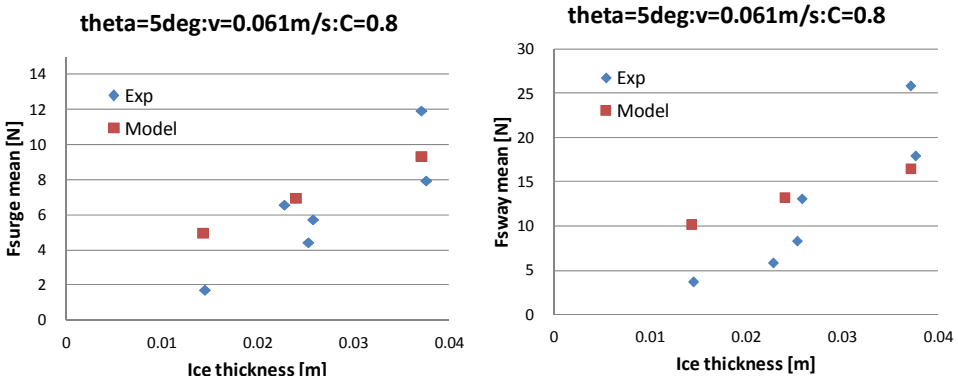

Figure 8. Comparison of surge and sway forces between measurements and predictions-2

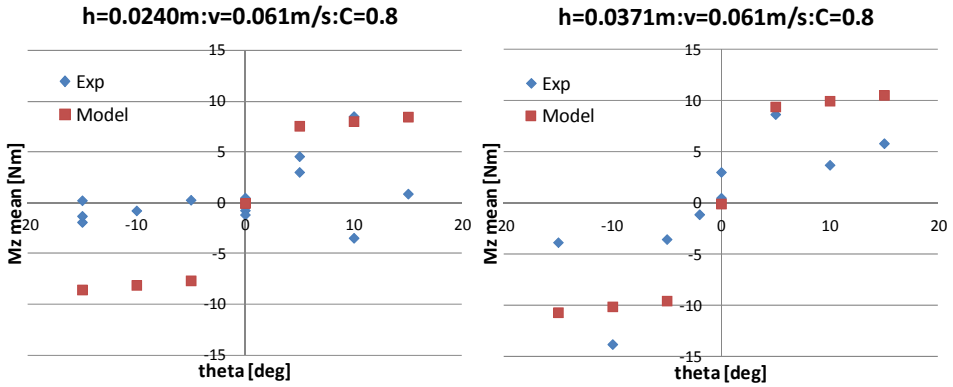

Figure 9. Comparison of yaw moment between measurements and prediction

DISCUSSIONS

Validity of the Simple Formula

In the present model, no local failure and submergence of ice floes are assumed. It means this model is fundamentally suitable for ships with a conventional, non-icebreaking hull form. As for the resistance in small ice floes, it was verified by the model experiments at the ice model basin (Uto et al., 2015). The surge force is not sensitive to the drift angle if the angle is small. Thus the validity of the present model is verified to some extent for the surge force.

It should also be noted that the validity of this model is confirmed for ice concentration of up to 0.8. It is reported that the original resistance model predicts higher resistance in small floes than the measured full-scale resistance in case of higher ice concentration. This is due to the contribution of local ice failure under such condition (Uto et al., 2015). Further validation is indispensable for the application to the severe ice conditions. In spite of these restrictions, the model is useful in the initial design of thruster sizing of the drillship in ice as well as the modeling of ice loads for the DP simulator in ice.

Ice force index for the DP operation

Figure 10 shows the fraction of each component of surge and sway forces. It clearly shows that the static component (no speed dependency, equations (4) and (9)) is dominant, particularly in the sway force. One of the reasons is low drift speed of ice.

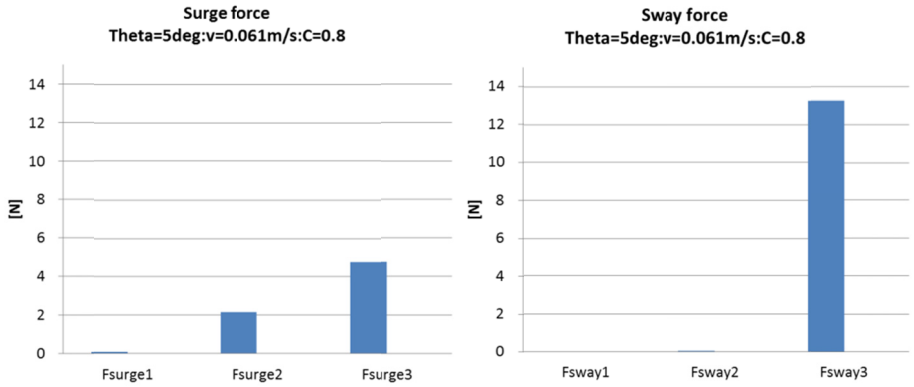

Figure 10. Fraction of each component of surge and sway forces

From equation (9), we obtained the following expression.

$$\widetilde{F}_{sway} = \frac{F_{Sway3}}{BL} = \frac{1}{2}\rho_i g\bar{k}_1\sqrt{d_i h_i}\,\frac{\left[(\frac{B_1}{2})^2(\mu + 4C_{WE1}\frac{L_{H1}}{B_1}) - (\frac{B_2}{2})^2(\mu_T + 4C_{WE2}\frac{L_{H2}}{B_2})\right]}{BL}$$
$$= \frac{1}{2}\rho_i g\bar{k}_1\sqrt{d_i h_i} \times f(Waterline\ shape, \mu, \theta) \qquad (12)$$

The first factor of the right hand side of equation (12) consists of only ice parameters. By normalizing with the values at C=0.8, h_i=1.0m and d_i=20m, we propose the following expression as the ice load index.

$$Index = \frac{\rho_i g\bar{k}_1\sqrt{d_i h_i}}{\rho_i g\bar{k}_1\sqrt{d_i h_i}_{\,C=0.8, hi=1.0, di=20m}} \qquad (13)$$

Figure 11 shows the relation of ice load index to size, concentration and thickness of ice floes. Index increases as the square root of ice thickness and floe size and the second-order polynomial of ice concentration (equation (5)). The top left figure indicates index decreases about 60 % (1.58 to 1.00) if the average floe size decreases from 50m to 20m. This index is also applicable for the effectiveness of physical ice management operation by icebreakers.

CONCLUSIONS

Model experiments were conducted at the ice model basin of the National Maritime Research Institute to measure ice loads exerted on the ship-shaped floating platform. We simulated managed ice floes encountering the model drillship with small drift angle and at low speed. Numerical simulation by physically-based modeling was also conducted indicating the reasonable agreement on surge and sway forces with the experimental data.

We also developed a simple analytical formula by extending the model by Kashitelijan, Poznjok and Ryblin, which was originally developed as the resistance model in small floes. The model gives reasonable agreement with measured ice forces and moment. Finally we propose the ice load index expressing the severity of DP operations in managed ice condition and the effectiveness of physical ice management operation by icebreakers.

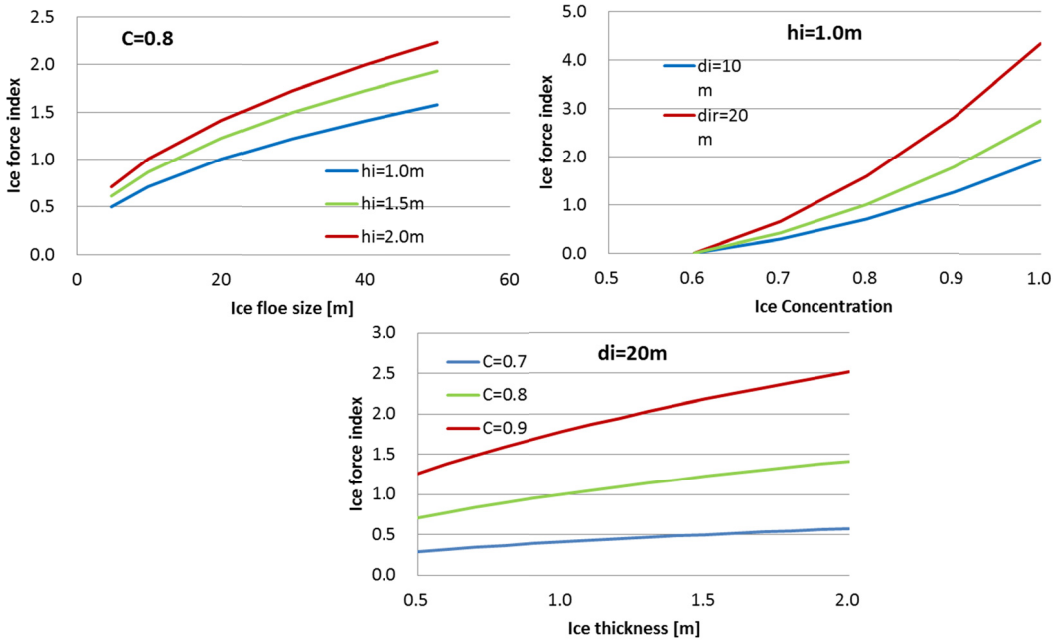

Figure 11. Ice load index vs. size, concentration and thickness of ice floe

REFERENCES

Bakkay, B.E., Coche, E. and Riska, K., 2014. Efficiency of Ice Management for Arctic Offshore Operations, Proceedings of the 33rd International Conference on Ocean, Offshore and Arctic Engineering (OMAE2014), pp.8

Haase, A. and Jochmann, P., 2013. DYPIC - Dynamic Positioning in Ice –Second Phase of Model Testing, Proceedings of the 32nd International Conference on Ocean, Offshore and Arctic Engineering (OMAE2013), pp.10

Izumiyama, K, Wako, D. Shimoda, H. and Uto, S., 2005. Ice Load Measurement on a Model ShipHull. Proceedings of the 18th International Conference on Port and Ocean Engineering under Arctic Conditions (POAC2005), Vol. 2, pp.635-645

Jensen, N.A., et al., 2009. DP in Ice Conditions, Proceedings of Dynamic Positioning Conference, pp.10

Keinonen, A.J.. et al., 2006. Transit and Stationary Coring Operations in the Central Polar Pack, Proceedings of the 7th International Conference and Exhibition on Performance of Ships and Structures in Ice (ICETEC) , pp.8

Kerkeni, S., Metrikin, I. and Jochmann, P., 2013. Capability Plots of Dynamic Positioning in Ice, Proceedings of the 32nd International Conference on Ocean, Offshore and Arctic Engineering (OMAE2013), pp.8

Konno, A., Nakane, A. and Kanamori, S., 2013. Validation of Numerical Estimation of Brash Ice Channel Resistance with Model Test, Proceedings of the 22nd International Conference on Port and Ocean Engineering under Arctic Conditions (POAC2013), pp.8

Metrikin, I., et al., 2012. Numerical Simulation of a Floater in a Broken-Ice Field – Part II: Comparative Study of Physics Engine, Proceedings of the 31st International Conference on Ocean, Offshore and Arctic Engineering (OMAE2012), pp.10

Nozawa, K., 2006. Ice Engineering (in Japanese). Seizando-Shoten Publishing Co.Ltd, pp.206-213.

Uto, S., Shimoda, H., Wako, D. and Matsuzawa, T., 2015. NSR Transit Simulations by the Vessel Performance Simulator “VESTA”, Part 2 Simple Resistance Formulae of Ships in Floe Ice, Proceedings of the 23rd International Conference on Port and Ocean Engineering under Arctic Conditions (POAC2015)